Title

Hydrogen sulfide induces Ca^{2+} release from the endoplasmic reticulum and suppresses ATP-induced Ca^{2+} signaling in rat spinal cord astrocytes

Takeshi Nii[a], Ryota Eguchi[a], Soichiro Yamaguchi[a], Ken-ichi Otsuguro[a]

[a]Laboratory of Pharmacology, Department of Basic Veterinary Sciences, Faculty of Veterinary Medicine, Hokkaido University, Kita 18, Nishi 9, Kita-ku, Sapporo 060-0818, Japan.

Corresponding author: K Otsuguro

Tel/Fax: +81-11-706-5220; E-mail: otsuguro@vetmed.hokudai.ac.jp

ORCID number: 0000-0002-2481-5592

Declarations of interest: none

Abstract

Hydrogen sulfide (H_2S) has a variety of physiological functions. H_2S reportedly increases intracellular Ca^{2+} concentration ($[Ca^{2+}]_i$) in astrocytes. However, the precise mechanism and functional role of this increase are not known. Here, we examined the effects of H_2S on $[Ca^{2+}]_i$ in astrocytes from the rat spinal cord and whether H_2S affects ATP-induced Ca^{2+} signaling, which is known to be involved in synaptic function. Na_2S (150 μM), an H_2S donor, produced a nontoxic increase in $[Ca^{2+}]_i$. The $[Ca^{2+}]_i$ increase by Na_2S was inhibited by Ca^{2+} depletion in the endoplasmic reticulum (ER) but not by removal of extracellular Ca^{2+}, indicating that H_2S releases Ca^{2+} from the ER. On the other hand, Na_2S inhibited ATP-induced $[Ca^{2+}]_i$ increase when Na_2S clearly increased $[Ca^{2+}]_i$ in the astrocytes, which was not suppressed by a reducing agent. In addition, Na_2S had no effect on intracellular cyclic AMP (cAMP) level. These results indicate that oxidative post-translational modification of proteins and cAMP are not involved in the inhibitory effect of H_2S on ATP-induced Ca^{2+} signaling. We conclude that H_2S indirectly inhibits ATP-induced Ca^{2+} signaling by decreasing Ca^{2+} content in the ER in astrocytes. In this way, H_2S may influence intercellular communication between astrocytes and neurons, thereby contributing to neuronal signaling in the nervous system.

Key words: hydrogen sulfide, ATP, calcium, astrocytes

1. Introduction

Hydrogen sulfide (H_2S) is a gaseous substance that is soluble in water (Filipovic et al., 2018). Under physiological conditions, approximately 20% of H_2S exists as a gas (Kimura, 2014). H_2S is transported across the cell membrane by simple diffusion (Mathai et al., 2009). At high concentrations, H_2S is well-known as a toxic gas because of the inhibitory effect on the mitochondrial electron transport chain (Cooper and Brown, 2008).

Despite the toxicity, low concentrations of H_2S is endogenously produced in several tissues, and is known to be one of the physiologically active substances (Kimura, 2014). H_2S modulates the structure and function of proteins by covalent modification of cysteine residues (Kimura, 2014), which is called *S*-sulfhydration (Mustafa et al., 2009). In *S*-sulfhydration, H_2S generates polysulfane (H_2S_n), which reacts with protein cysteine residues (Liu et al., 2018). In addition, H_2S exerts its biological functions by changing the concentration of intracellular cyclic AMP (cAMP) (Cao et al., 2018). The increase of cAMP by H_2S is reported to activate ion channels through protein kinase A-dependent phosphorylation (Perniss et al., 2017).

In the central nervous system (CNS), H_2S is produced mainly by astrocytes (Lee et al., 2009). In the hippocampal astrocytes, H_2S is shown to increase intracellular Ca^{2+} concentration ($[Ca^{2+}]_i$), which is caused mainly by Ca^{2+} influx through the transient receptor potential (TRP) A1 channels via *S*-sulfhydration (Kimura et al., 2013; Nagai et al., 2004;

Ogawa et al., 2012). It is also reported that H_2S causes Ca^{2+} release from the intracellular Ca^{2+} stores, but its mechanism and functional significance in the CNS are still unknown.

The increase in $[Ca^{2+}]_i$ contributes to intercellular communication between astrocytes and surrounding neurons (Guerra-Gomes et al., 2018; Scemes and Giaume, 2006). $[Ca^{2+}]_i$ in astrocytes is also increased in response to neurotransmitters, such as adenosine 5′-triphosphate (ATP), which activates P_2 purinoreceptors and stimulates inositol 1,4,5-triphosphate (IP_3) signaling, resulting in the release of Ca^{2+} from the ER through IP_3 receptor activation (Guthrie et al., 1999; Salter and Hicks, 1995, 1994). The ATP-induced $[Ca^{2+}]_i$ increase in astrocytes is reported to regulate synaptic functions (Domercq et al., 2006; Navarrete et al., 2013) and may contribute to early symptoms of disease in the CNS (Agulhon et al., 2012). Therefore, the factors regulating Ca^{2+} signaling by ATP in astrocytes are expected to be a useful target for developing the new therapeutic strategy.

We report here that H_2S induces Ca^{2+} release from the ER in rat spinal cord astrocytes. The depletion of Ca^{2+} in the ER by H_2S suppresses ATP-induced Ca^{2+} signaling. Our data demonstrate that *S*-sulfhydration and intracellular cAMP do not contribute to this inhibitory effect by H_2S.

2. Materials and Methods

2.1. Reagents

Dithiothreitol (DTT), 2-aminoethoxydiphenylborane (2APB), and allyl isothiocyanate (AITC) were purchased from FUJIFILM Wako Pure Chemicals Industries (Osaka, Japan). ATP disodium salt hydrate and cremophor EL were purchased from Sigma-Aldrich (St.Louis, MO). Na_2S, Na_2S_3, 1-[6-amino-2-(5-carboxy-2-oxazolyl)-5-benzofuranyloxy]-2-(2-aminom-5-methylphenoxy) ethane-*N*,*N*,*N*',*N*'-tetraacetic acid, pentaacetoxymethyl ester (Fura-2 AM), and *O*,*O'*-bis(2-aminoethyl)ethylene-glycol-*N*,*N*,*N*',*N*'-tetraacetic acid (EGTA) were purchased from Dojindo (Kumamoto, Japan). Theophylline-7-(*N*-4-isopropylphenyl) acetamide (HC-030031) was purchased from Tocris (Bristol, UK). Thapsigargin and 1-[6-[[(17β)-3-methoxyestra-1,3,5(10)-trien-17-yl]amino]hexyl]-1H-pyrrole-2,5-dione (U73122) was purchased from Cayman Chemicals (An Arbor, MI). Ryanodine was purchased from Abcam (Cambridge, UK).

2.2. Animals

Wistar rats were obtained from Clea Japan (Tokyo, Japan). The animals had *ad libitum* access to food and tap water, and were maintained in a temperature-controlled environment on a 12:12 h light/dark cycle. Male and female pups aged 0−3 days were used

for experiments. All animal care and experimental protocols were approved by the Committee on Animal Experimentation, Graduate School of Veterinary Medicine, Hokkaido University (no. 19-0009).

2.3. Cell cultures

Cultured astrocytes of the spinal cord were obtained from Wistar rats. Neonatal rats were killed by decapitation and the isolated spinal cord was minced in divalent cation-free Hanks' balanced salt solution. Following digestion with papain (10 U/ml) and DNase (0.1 mg/ml) at room temperature for 20 min, tissues were mechanically dissociated with a Pasteur pipette in culture medium. The culture medium was Dulbecco's modified Eagle Medium (DMEM)/Ham's-F12 containing 10% fetal bovine serum (FBS), 100 U/ml penicillin, and 0.1 mg/ml of streptomycin. The cell suspension was transferred to a poly-L-lysine-coated T75 flask, and the medium was replaced after 1−2 h. Cells were cultured in a humidified environment containing 5% CO_2 at 37°C and the culture medium was replaced every 2 or 3 days. When cells reached 80 − 90% confluence, flasks were shaken vigorously at 250 rpm for at least 12 h to remove nonadherent cells. The remaining astrocytes were trypsinized and seeded in poly-L-lysine-coated T25 flasks, microwell plates, dishes, or cover glasses (Φ15). All cells were positive for the astrocyte marker glial fibrillary acidic protein (Eguchi et al., 2015).

2.4. Calcium imaging

The cells were seeded on cover glasses at a density of 5×10^3 cells/cm^2 and cultured for 9−15 days. The cells were then washed with artificial cerebrospinal fluid (ACSF; 138 mM NaCl, 3.5 mM KCl, 1.25 mM $CaCl_2$, 1.2 mM $MgCl_2$, 25 mM HEPES, and 10 mM glucose, pH 7.3 with NaOH) and loaded with 10 μM Fura-2 AM and 0.002% (v/v) cremophor EL in ACSF for 60 min at 37°C. Fura-2 fluorescence was measured using an inverted microscope (Diaphot 300, Nikon, Tokyo, Japan) with a fluorescence ratio imaging system (ORCA-ER; Hamamatsu Photonics, Shizuoka, Japan). Cells were continuously superfused with ACSF and illuminated at 340 and 380 nm for 111 ms at 2 s intervals. The respective fluorescence signals (F_{340} and F_{380}) were detected at 500 nm. The ratio of F_{340} and F_{380} (R) was analyzed after correction of background fluorescence using Aquacosmos 2.6 software (Hamamatsu Photonics). The intracellular calcium concentration ($[Ca^{2+}]_i$) was calculated using the following equation : $[Ca^{2+}]_i = K_D\beta \times (R—R_{min})/(R_{max}-R)$ (Grynkiewicz et al., 1985). The dissociation constant of Fura-2 and Ca^{2+} (K_D), the ratio of F_{380} at saturating Ca^{2+} to F_{380} at zero Ca^{2+} (β), and the minimum (R_{min}) and maximum (R_{max}) of the fluorescence ratio (F_{340}/F_{380}) were calculated using a Calcium Calibration Buffer kit (Invitrogen, Carlsbad, CA). All experiments were performed at room temperature. To remove extracellular Ca^{2+}, $CaCl_2$ in ACSF was replaced with 1 mM EGTA.

Basal $[Ca^{2+}]_i$ was determined from a single point just before application of drugs unless otherwise stated. Peak $[Ca^{2+}]_i$ was determined from a single maximum point during application of drugs. The peak amplitude was calculated as the difference between peak $[Ca^{2+}]_i$ and basal $[Ca^{2+}]_i$.

2.5. Viability analysis

The cells were seeded on 96-well plates at a density of 1×10^4 cells/cm^2 and incubated for 2 h with medium containing 1% fetal bovine serum. After washing once, cells were treated with Na_2S (1 μM − 1 mM) for 6 h. Lactate dehydrogenase (LDH) release from astrocytes was assessed with the Cytotoxicity Detection LDH kit (Roche, Indianapolis, IN) according to the manufacturer's instructions. Absorbance at 490 nm was measured by a microplate reader (SH-1000; Corona Electric, Hitachinaka, Japan) with the correction set at 700 nm.

2.6. Cell proliferation assay

The cells were seeded at a density of 1×10^4 cells/cm^2 on 96-well plates and incubated for 24 h with medium containing 10% fetal bovine serum. After incubation, astrocytes were treated with Na_2S (150 μM) for 24 h, after which the medium was discarded and 100 μl fresh medium was added. Cell proliferation was assessed with a

3-[4,5-dimethylthiazolyl-2]-2,5-diphenyltetrazolium bromide (MTT) assay using MTT Cell Count kit (Nacalai Tesque, Kyoto, Japan) according to the manufacturer's instructions. Absorbance was measured at 570 nm on a microplate reader with the correction set at 650 nm.

2.7. Measurement of ATP release

The cells were plated at a density of 1.5×10^4 cells/cm^2 on 24-well plates. Once the cells reached confluence, they were incubated with ACSF (37°C) for 1 h before Na_2S (final concentrations, 0.001–150 μM) was added. Na_2S was applied by dropping a highly concentrated solution. Five minutes later, samples (50 μl) were collected and boiled. Remaining cells were suspended in 0.1 N NaOH and sonicated. The protein content of cell lysates was measured using the Quick Start protein assay (Bio-Rad, Hercules, CA). ATP in the samples was measured with the luciferin-luciferase technique using the ATP Determination kit (Invitrogen) and a microplate reader (SH-9000; Corona Electric). A calibration curve was prepared using standard solutions containing known concentrations of ATP, and concentrations of ATP in the samples were calculated from it. The amounts of ATP were expressed as the extracellular amount per milligram of protein in cell lysates (pmol/mg protein).

2.8. cAMP assay

The cells were seeded at a density of 5×10^3 cells/cm^2 in 60 mm dishes and cultured for 10−14 days before experiments. The cells were washed and then incubated in ACSF for 60 min at 37°C. After the incubation, cells were brought to room temperature and treated with Na_2S (150 μM), Na_2S_3 (10 μM), or forskolin (100 μM) for 10 min. Control samples were treated for 10 min with an appropriate volume of vehicle (distilled water). The ACSF was then aspirated and cells were treated with HCl (0.1 M) for 20 min at room temperature. Cells were scraped from dishes and then centrifuged at 1,000 × g for 10 min. The supernatants were used for measurement of cAMP content with a cAMP enzyme immunoassay kit (Cayman Chemicals).

2.9. Statistical analysis

Data are expressed as means ± standard errors of the means (S.E.M.). Statistical comparisons between two groups were assessed using Student's *t*-tests, and analyses of variance followed by Dunnett's tests were used for multiple comparisons. A P-value < 0.05 was considered significant. Ekuseru–Toukei 2008 statistical software (Social Survey Research Information Co., Ltd., Tokyo, Japan) was used for all statistical analyses.

3. Results

3.1. H_2S increases $[Ca^{2+}]_i$ in spinal cord astrocytes.

First, we measured the effect of H_2S on $[Ca^{2+}]_i$ levels in cultured spinal cord astrocytes. The basal $[Ca^{2+}]_i$ levels were 38.3 ± 1.3 nM (n = 379 cells from 3 cultures), and the application of Na_2S at more than 100 μM for 10 min significantly increased $[Ca^{2+}]_i$ (n = 89-100 cells from 3 cultures, Fig. 1A, B). The $[Ca^{2+}]_i$ recovered to nearly basal level 3 min after removal of Na_2S at 100 μM, but not at 1 mM ($\Delta[Ca^{2+}]_i$ at 0 μM : 8.98 ± 1.24 nM, 100 μM : 15.40 ± 2.99 nM, and 1 mM : 67.61 ± 7.41 nM, $P < 0.01$ vs. 0 μM Na_2S Dunnett's test, n = 93-100 cells from 3 cultures).

To determine if the concentrations of Na_2S used in our study caused damage to astrocytes, we incubated cells with various concentrations of Na_2S (1 μM−1 mM) for 6 h and assessed the level of the extracellular lactate dehydrogenase which is rapidly released from damaged cells. As the result, no increase in lactate dehydrogenase release was observed (Fig. 1C). Furthermore, incubation with Na_2S (150 μM) for 24 h did not affect cell viability in MTT assay (Fig. 1D), demonstrating that Na_2S is not toxic at concentrations up to 150 μM. As physiological concentrations of H_2S in the brain are 50−166 μM (Baskar and Bian, 2011), we used Na_2S at concentrations ≤150 μM in subsequent experiments.

3.2. H_2S inhibits ATP-induced $[Ca^{2+}]_i$ increase in astrocytes.

The application of ATP (10 μM) for 30 s increased $[Ca^{2+}]_i$ (ΔATP_1) in almost all cells (Fig. 2A). ATP induced transient $[Ca^{2+}]_i$ increase and there was a plateau in some cells after the application of ATP. This ATP-induced $[Ca^{2+}]_i$ increase was almost completely inhibited after incubation with U73122 (5 μM, 60 min), a phospholipase C inhibitor (Fig. S1A), suggesting that ATP (10 μM) induces mainly Ca^{2+} release from the ER through IP_3 signaling pathway in spinal cord astrocytes. Fifteen minutes after the first application, the second application of ATP also increased $[Ca^{2+}]_i$ (ΔATP_2), and the ratio of the second ATP-induced $[Ca^{2+}]_i$ increase to the first one ($\Delta ATP_2/\Delta ATP_1$) was consistent. Then we examined the effects of H_2S on ATP-induced Ca^{2+} response in spinal cord astrocytes. After the first application of ATP, cells were treated with Na_2S (0.1−150 μM) for 10 min, and the second application of ATP was done in the presence of Na_2S. After the first application of ATP, Na_2S at more than 100 μM increased $[Ca^{2+}]_i$ (Fig. 2A, B). Furthermore, $\Delta ATP_2/\Delta ATP_1$ decreased in the presence of Na_2S at more than 100 μM(Fig. 2A, C). These results suggest that the suppression of ATP signaling is related to H_2S-induced $[Ca^{2+}]_i$ increase.

Increases in $[Ca^{2+}]_i$ trigger the exocytosis of ATP from astrocytes (Pryazhnikov and Khiroug, 2008), thus increases in $[Ca^{2+}]_i$ by H_2S might induce ATP release from astrocytes. However, the application of Na_2S (0.001−150 μM, 5 min) did not alter the extracellular concentrations of ATP (Fig. 2D), suggesting that H_2S-induced $[Ca^{2+}]_i$ increase does not promote the exocytosis of ATP.

3.3. Ca^{2+} response to H_2S does not depend on Ca^{2+} influx in spinal cord astrocytes.

We next examined the mechanism of H_2S-induced $[Ca^{2+}]_i$ increase. In rat hippocampal astrocytes, it was reported that H_2S increases $[Ca^{2+}]_i$ via the activation of TRPA1. However, the $[Ca^{2+}]_i$ increase by Na_2S (150 μM) was not suppressed by HC-030031 (10 μM), a selective TRPA1 inhibitor (McNamara et al., 2007) (Fig. 3A), and allyl isothiocyanate (AITC, 10 μM), a TRPA1 agonist (McNamara et al., 2007), did not increase $[Ca^{2+}]_i$ (Fig. 3B). Furthermore, removal of extracellular Ca^{2+} by replacing $CaCl_2$ in ACSF with 1 mM EGTA did not decrease $[Ca^{2+}]_i$ increase by Na_2S (Fig. 3C). These results indicate that H_2S-induced $[Ca^{2+}]_i$ increase does not depend on the activity of TRPA1 or Ca^{2+} influx in rat spinal cord astrocytes.

3.4. H_2S induces Ca^{2+} release from the ER in astrocytes.

We examined whether H_2S induces Ca^{2+} release from intracellular Ca^{2+} stores. The application of thapsigargin (1 μM), which depletes Ca^{2+} in the ER by inhibiting sarco/endoplasmic reticulum Ca^{2+}-ATPase (SERCA) (Thastrup et al., 1990), increased the $[Ca^{2+}]_i$ (Fig. 4A). In the presence of thapsigargin, Na_2S-induced $[Ca^{2+}]_i$ increase markedly decreased (Fig. 4A, B).

Next, we examined whether the decrease of Ca^{2+} in the ER by ATP affects the

H_2S-induced $[Ca^{2+}]_i$ increase. Repetitive application of ATP (10 μM, 30 s) increased $[Ca^{2+}]_i$ each time in the presence of extracellular Ca^{2+} (Fig. 4C), indicating that Ca^{2+} was taken into the ER and the Ca^{2+} content in the ER was maintained. Under the Ca^{2+} free condition, $[Ca^{2+}]_i$ increase by the second application of ATP markedly decreased ($\Delta ATP_2/\Delta ATP_1$, control: 0.79 ± 0.02, n = 87, vs. Ca^{2+} free: 0.46 ± 0.03, n = 76, $P < 0.01$, unpaired Student's t-test), and then the Ca^{2+} response to Na_2S (150 μM, 10 min) after the second application of ATP was almost abolished (Fig. 4D, E). These results suggest that ATP and H_2S mobilize Ca^{2+} from the same ER.

Ca^{2+} is released from the ER by changes in the activities of IP_3 receptors, ryanodine receptors, and SERCA. We examined whether H_2S induces the release of Ca^{2+} from the ER through IP_3 receptors. The application of 2-aminoethoxydiphenyl borate (2APB) (100 μM, 2 min), which is a general inhibitor of IP_3 receptors (Peppiatt et al., 2003), slightly increased $[Ca^{2+}]_i$ by itself and decreased $\Delta ATP_2/\Delta ATP_1$ (Fig. S2A, B). 2APB did not completely suppress ATP-induced Ca^{2+} response. This inhibitory effect of 2APB did not change with extended application time (10 min). This is probably because a subtype of IP_3 receptors expressed in spinal cord astrocytes is less sensitive to 2APB (Saleem et al., 2014). Therefore, we did not investigate the effect of 2APB on H_2S-induced $[Ca^{2+}]_i$ increase. Then, we examined the effect of U73122, a phospholipase C inhibitor, on the H_2S-induced $[Ca^{2+}]_i$ increase. U73122 (5 μM, 60 min) did not inhibit, but enhanced $[Ca^{2+}]_i$ increase by Na_2S (Fig.

S1B), suggesting that IP_3 signaling pathway is not involved in H_2S-induced $[Ca^{2+}]_i$ increase.

Next, we examined whether ryanodine receptors are involved in H_2S-iduced $[Ca^{2+}]_i$ increase. The high concentrations of ryanodine inhibit opening of ryanodine receptors (Willmott et al., 2000). The $[Ca^{2+}]_i$ increase by ryanodine (1 μM) was inhibited after incubation with ryanodine (100 μM, 30 min, Fig. S3A). Under the same conditions, the peak amplitude of Ca^{2+} increase by Na_2S (150 μM, 5 min) was 75.9 ± 6.4 nM (n = 99 cells from 3 cultures) (Fig. S3B). The $[Ca^{2+}]_i$ increase by Na_2S was not inhibited by the pretreatment of ryanodine (Fig. 4B), suggesting that H_2S does not release Ca^{2+} from the ER through ryanodine receptors.

3.5. H_2S induces Ca^{2+} responses via *S*-sulfhydration-independent mechanism.

To determine if *S*-sulfhydration of proteins contributes to H_2S-induced $[Ca^{2+}]_i$ increase in astrocytes, we applied 1 mM DTT, a reducing agent that can reverse covalent *S*-sulfhydration modifications (Cooper and Brown, 2008). DTT not only failed to suppress the H_2S-induced $[Ca^{2+}]_i$ increase, but slightly increased it (Fig. 5A). DTT also did not affect the inhibitory effect of H_2S on ATP-induced $[Ca^{2+}]_i$ increase (Fig. 5B, C). We next tested the effects of Na_2S_3, a donor of H_2S_n, that induces *S*-sulfhydration at low concentrations (Kimura et al., 2013). Na_2S_3 (0.1−10 μM) slightly increased $[Ca^{2+}]_i$ but inhibited the ATP-induced $[Ca^{2+}]_i$ increase only at the lowest concentration (0.1 μM) (Fig. 5D-F). These results indicate

that H_2S-induced $[Ca^{2+}]_i$ increase is largely independent of *S*-sulfhydration.

3.6. Ca^{2+} responses induced by H_2S do not depend on cAMP.

H_2S also alters intracellular levels of cAMP, which regulates the various cell functions (Cao et al., 2018). Generally, cAMP activates protein kinase A, which modulates the activities of Ca^{2+} channels on the ER membrane (Desouza et al., 2002; Zalk et al., 2007). Na_2S (150 μM) or Na_2S_3 (10 μM) treatment for 10 min failed to alter the intracellular concentration of cAMP, while forskolin (100 μM), an adenylate cyclase agonist, increased cAMP levels (Fig. 5G). These results suggest that cAMP is not involved in H_2S-induced $[Ca^{2+}]_i$ increase.

4. Discussion

H_2S is shown to increase $[Ca^{2+}]_i$ in astrocytes, but its mechanism and role are not clear. Extracellular ATP is major mediator of Ca^{2+} signals in astrocytes (Guthrie et al., 1999), which regulates communication between astrocytes and surrounding cells including other astrocytes and neurons (Guerra-Gomes et al., 2018). In this study, we demonstrated that H_2S induces Ca^{2+} release from the ER, and inhibits ATP-induced $[Ca^{2+}]_i$ increase in spinal cord astrocytes.

In rat hippocampal astrocytes, H_2S induces Ca^{2+} influx via *S*-sulfhydration of TRPA1 (Kimura et al., 2013; Nagai et al., 2004), which occurs with low concentrations of polysulfane donors, such as Na_2S_3 (EC_{50} 91 nM), and is reversed by DTT (Kimura et al., 2013; Ujike et al., 2015). However, in the present study, H_2S-induced $[Ca^{2+}]_i$ increase was not affected by a TRPA1 antagonist, DTT, or removal of extracellular Ca^{2+}. Furthermore, AITC, a TRPA1 agonist, did not induce clear $[Ca^{2+}]_i$ increase. Several previous studies suggest that H_2S also acts on transient receptor potential vanilloid 1 (TRPV1) (Krueger et al., 2010; Trevisani et al., 2005). However, recent studies show that H_2S does not directly activate TRPV1 (Miyamoto et al., 2011; Ogawa et al., 2012). Taken together, it is considered that TRPA1 and TRPV1 are not involved in H_2S-induced $[Ca^{2+}]_i$ increase in rat spinal cord astrocytes.

H_2S-induced $[Ca^{2+}]_i$ increase was suppressed by thapsigargin, a SERCA inhibitor, and by the depletion of Ca^{2+} content in the ER after the application of ATP in the absence of

extracellular Ca^{2+}. Moreover, H_2S inhibited ATP-induced $[Ca^{2+}]_i$ increase, suggesting that both H_2S and ATP release Ca^{2+} from the same ER. The release of Ca^{2+} from the ER by H_2S has been reported in several different cells (Bauer et al., 2010; de Pascual et al., 2018; Yong et al., 2010). These reports also show that depletion of Ca^{2+} in the ER by SERCA inhibitors or the stimulation of IP_3 receptors suppresses H_2S-induced $[Ca^{2+}]_i$ increase. The inhibitory effect of H_2S on ATP-induced $[Ca^{2+}]_i$ increase in the absence of extracellular Ca^{2+} was also reported in human vascular endothelial cells (Bauer et al., 2010). On the other hand, in SH-SY5Y cells, H_2S increases $[Ca^{2+}]_i$ by Ca^{2+} release from the ER and Ca^{2+} influx via protein kinase A pathway (Yong et al., 2010). As mentioned above, in the present study, H_2S did not induce Ca^{2+} influx and intracellular cAMP elevation in spinal cord astrocytes.

The ATP-induced $[Ca^{2+}]_i$ increase was inhibited when H_2S clearly induced $[Ca^{2+}]_i$ increase by Na_2S at more than 100 μM. This result indicates a strong relationship between the $[Ca^{2+}]_i$ increase and the inhibition of ATP-induced Ca^{2+} signals by H_2S. $[Ca^{2+}]_i$ directly regulates Ca^{2+} release through IP_3 receptors on the ER membrane (Hno, 1990): $[Ca^{2+}]_i$ between 0 and 300 nM activates IP_3 receptors, whereas >300 nM $[Ca^{2+}]_i$ inhibits them. In this study, the resting $[Ca^{2+}]_i$ in cultured astrocytes was around 100 nM, and Na_2S (150 μM) increased $[Ca^{2+}]_i$ by approximately 50 nM. Thus, it is unlikely that H_2S-induced $[Ca^{2+}]_i$ increase inhibited IP_3 receptors. On the other hand, H_2S may have depleted the Ca^{2+} content in the ER, thereby preventing subsequent ATP-induced $[Ca^{2+}]_i$ increases. Further studies are

needed to elucidate the mechanism underlying H_2S-induced Ca^{2+} release from the ER. We found that ryanodine receptors are not major Ca^{2+} transporting proteins activated by H_2S in spinal cord astrocytes, but it is not known if H_2S directly affects the activities of other Ca^{2+} leak channels and/or SERCA.

H_2S_n derived from H_2S modifies cysteine residues of proteins and modulates their functions (Kimura, 2014). This *S*-sulfhydration is an oxidative reaction (Lau and Pluth, 2019) and is one of the most important biological functions of H_2S. Plasma membrane ATP-sensitive K^+ (KATP) channels are activated by *S*-sulfhydration, which is reversed by DTT (Kang et al., 2015). The activation of KATP channels suppresses Ca^{2+} influx by hyperpolarization of the plasma membrane (Ashcroft, 2005). In this study, DTT did not inhibit the effect of H_2S on $[Ca^{2+}]_i$, suggesting that the oxidative reaction is not involved. KATP channels are also expressed in mitochondria. It is speculated that mitochondrial KATP channels have different structure and properties from those expressed on the cell membrane (Huang et al., 2019). Opening of mitochondrial KATP channels has been reported to induce Ca^{2+} release from mitochondria (Holmuhamedov et al., 1999). Although it has been suggested that H_2S acts on mitochondrial KATP channels (Testai et al., 2016), it is unclear whether H_2S mobilizes intracellular Ca^{2+} through the regulation of mitochondrial KATP channels. Further studies should be conducted to reveal the action of H_2S on mitochondrial KATP channels.

H_2S affects intracellular respiration by inhibiting cytochrome *c* oxidase in

mitochondria or by supplying electrons to facilitate its activity (Cooper and Brown, 2008; Szabo et al., 2014). Inhibition of the electron transport chain depolarizes the mitochondrial membrane potential (Barrientos and Moraes, 1999), which releases Ca^{2+} from the mitochondrial matrix (Zhao et al., 2013). The mitochondrial depolarization by H_2S is also reported (Eghbal et al., 2004). In this study, the depletion of Ca^{2+} content in the ER by thapsigargin did not completely suppress H_2S-induced $[Ca^{2+}]_i$ increase. Therefore, it is presumed that H_2S acts on other Ca^{2+} stores including mitochondria. In bovine adrenal chromaffin cells, H_2S is suggested to release Ca^{2+} from the ER and mitochondria (de Pascual et al., 2018). Furthermore, changes in intracellular respiration caused by H_2S influence the concentrations of bioactive substances including ATP, reactive oxygen species, and NADH, which modulate the activities of Ca^{2+} transporting proteins on the ER membranes (Chernorudskiy and Zito, 2017; Kaplin et al., 1996). It is worth examining whether H_2S changes intracellular respiration and whether its products are involved in H_2S-induced $[Ca^{2+}]_i$ increase in future studies.

In conclusion, H_2S induces Ca^{2+} release from the ER and inhibits ATP-induced $[Ca^{2+}]_i$ increase in astrocytes. This inhibition was attributed to the decrease of Ca^{2+} content in the ER. Astrocytes may be particularly vulnerable to these effects, as they are the main source of H_2S in the CNS. The present study suggests that H_2S can regulate intercellular communication between astrocytes and surrounding cells through Ca^{2+}. This is important

finding because pathological damage to the CNS increases extracellular ATP concentrations and, subsequent $[Ca^{2+}]_i$ increase in astrocytes leads to synaptic dysfunction (Agulhon et al., 2012). Our findings may lead to further research to reveal the relationship between H_2S and the progression of synaptic dysfunction under pathological conditions.

Declarations

Conflicts of interest/Competing interests: The authors declare that they have no conflicts of interest.

Acknowledgments: This work was supported by a Grant-in-Aid for Scientific Research from the Japan Society for the Promotion of Science [no. 19K23701]

References

Agulhon, C., Sun, M.Y., Murphy, T., Myers, T., Lauderdale, K., Fiacco, T.A., 2012. Calcium signaling and gliotransmission in normal vs. Reactive astrocytes. Front. Pharmacol. 3 JUL, 1–16. https://doi.org/10.3389/fphar.2012.00139.

Ashcroft, F.M., 2005. ATP-sensitive potassium channelopathies : focus on insulin secretion Find the latest version : Review series ATP-sensitive potassium channelopathies : focus on insulin secretion. J. Clin. Invest. 115, 2047–2058. https://doi.org/10.1172/JCI25495.

Barrientos, A., Moraes, C.T., 1999. Titrating the effects of mitochondrial complex I impairment in the cell physiology. J. Biol. Chem. 274, 16188–16197. https://doi.org/10.1074/jbc.274.23.16188.

Baskar, R., Bian, J., 2011. Hydrogen sulfide gas has cell growth regulatory role. Eur. J. Pharmacol. 656, 5–9. https://doi.org/10.1016/j.ejphar.2011.01.052.

Bauer, C.C., Boyle, J.P., Porter, K.E., Peers, C., 2010. Modulation of Ca^{2+} signalling in human vascular endothelial cells by hydrogen sulfide. Atherosclerosis 209, 374–380. https://doi.org/10.1016/j.atherosclerosis.2009.10.004.

Cao, X., Wu, Z., Xiong, S., Cao, L., Sethi, G., Bian, J. song, 2018. The role of hydrogen sulfide in cyclic nucleotide signaling. Biochem. Pharmacol. 149, 20–28. https://doi.org/10.1016/j.bcp.2017.11.011.

Chernorudskiy, A.L., Zito, E., 2017. Regulation of Calcium Homeostasis by ER Redox: A Close-Up of the ER/Mitochondria Connection. J. Mol. Biol. 429, 620–632. https://doi.org/10.1016/j.jmb.2017.01.017.

Cooper, C.E., Brown, G.C., 2008. The inhibition of mitochondrial cytochrome oxidase by the gases carbon monoxide, nitric oxide, hydrogen cyanide and hydrogen sulfide: chemical mechanism and physiological significance. J. Bioenerg. Biomembr. 40, 533–539. https://doi.org/10.1007/s10863-008-9166-6.

de Pascual, R., Baraibar, A.M., Méndez-López, I., Pérez-Ciria, M., Polo-Vaquero, I., Gandía, L., Ohia, S.E., García, A.G., de Diego, A.M.G., 2018. Hydrogen sulphide facilitates exocytosis by regulating the handling of intracellular calcium by chromaffin cells. Pflugers Arch. Eur. J. Physiol. 470, 1255–1270. https://doi.org/10.1007/s00424-018-2147-7.

Desouza, N., Reiken, S., Ondrias, K., Yang, Y.M., Matkovich, S., Marks, A.R., 2002. Protein kinase A and two phosphatases are components of the inositol 1,4,5-trisphosphate receptor macromolecular signaling complex. J. Biol. Chem. 277, 39397–39400. https://doi.org/10.1074/jbc.M207059200.

Domercq, M., Brambilla, L., Pilati, E., Marchaland, J., Volterra, A., Bezzi, P., 2006. P2Y1 receptor-evoked glutamate exocytosis from astrocytes: Control by tumor necrosis factor-α and prostaglandins. J. Biol. Chem. 281, 30684–30696.

https://doi.org/10.1074/jbc.M606429200.

Eghbal, M.A., Pennefather, P.S., O'Brien, P.J., 2004. H2S cytotoxicity mechanism involves reactive oxygen species formation and mitochondrial depolarisation. Toxicology 203, 69–76. https://doi.org/10.1016/j.tox.2004.05.020.

Eguchi, R., Akao, S., Otsuguro, K., Yamaguchi, S., Ito, S., 2015. Different mechanisms of extracellular adenosine accumulation by reduction of the external Ca^{2+} concentration and inhibition of adenosine metabolism in spinal astrocytes. J. Pharmacol. Sci. 128, 47–53. https://doi.org/10.1016/j.jphs.2015.04.008.

Filipovic, M.R., Zivanovic, J., Alvarez, B., Banerjee, R., 2018. Chemical Biology of H_2S Signaling through Persulfidation. Chem. Rev. 118, 1253–1337. https://doi.org/10.1021/acs.chemrev.7b00205.

Grynkiewicz, G., Poenie, M., Tsien, R.Y., 1985. A New Generation of Ca^{2+} Indicators with Greatly Improved Fluorescence Properties. J. Biol. Chem. 260, 3440–3450.

Guerra-Gomes, S., Sousa, N., Pinto, L., Oliveira, J.F., 2018. Functional roles of astrocyte calcium elevations: From synapses to behavior. Front. Cell. Neurosci. 11, 1–7. https://doi.org/10.3389/fncel.2017.00427.

Guthrie, P.B., Knappenberger, J., Segal, M., Bennett, M.V.L., Charles, A.C., Kater, S.B., 1999. ATP released from astrocytes mediates glial calcium waves. J. Neurosci. 19, 520–528. https://doi.org/10.1523/JNEUROSCI.19-02-00520.1999.

Hno, M., 1990. Biphasic Ca^{2+} dependence of inositol 1,4,5-trisphosphate-induced Ca release in smooth muscle cells of the guinea pig taenia caeci. J. Gen. Physiol. 95, 1103–1122. https://doi.org/10.1085/jgp.95.6.1103.

Holmuhamedov, E.L., Wang, L., Terzic, A., 1999. ATP-sensitive K^+ channel openers prevent Ca^{2+} overload in rat cardiac mitochondria. J. Physiol. 519, 347–360. https://doi.org/10.1111/j.1469-7793.1999.0347m.x.

Huang, Y., Hu, D., Huang, C., Nichols, C.G., 2019. Genetic Discovery of ATP-Sensitive K^+ Channels in Cardiovascular Diseases. Circ. Arrhythmia Electrophysiol. 12, 1–11. https://doi.org/10.1161/CIRCEP.119.007322.

Kang, M., Hashimoto, A., Gade, A., Akbarali, H.I., 2015. Interaction between hydrogen sulfide-induced sulfhydration and tyrosine nitration in the KATP channel complex. Am. J. Physiol. - Gastrointest. Liver Physiol. 308, G532–G539. https://doi.org/10.1152/ajpgi.00281.2014.

Kaplin, A.I., Snyder, S.H., Linden, D.J., 1996. Reduced nicotinamide adenine dinucleotide-selective stimulation of inositol 1,4,5-trisphosphate receptors mediates hypoxic mobilization of calcium. J. Neurosci. 16, 2002–2011. https://doi.org/ 10.1523/jneurosci.16-06-02002.1996.

Kimura, H., 2014. Hydrogen sulfide and polysulfides as biological mediators. Molecules. 19, 16146–16157. https://doi.org/10.3390/molecules191016146.

Kimura, Y., Mikami, Y., Osumi, K., Tsugane, M., Oka, J., Kimura, H., 2013. Polysulfides are possible H_2S-derived signaling molecules in rat brain. FASEB J. 27, 2451–2457. https://doi.org/10.1096/fj.12-226415.

Krueger, D., Foerster, M., Mueller, K., Zeller, F., Slotta-Huspenina, J., Donovan, J., Grundy, D., Schemann, M., 2010. Signaling mechanisms involved in the intestinal pro-secretory actions of hydrogen sulfide. Neurogastroenterol. Motil. 22. https://doi.org/10.1111/j.1365-2982.2010.01571.x.

Lau, N., Pluth, M.D., 2019. Reactive sulfur species (RSS): persulfides, polysulfides, potential, and problems. Curr. Opin. Chem. Biol. 49, 1–8. https://doi.org/10.1016/j.cbpa.2018.08.012.

Lee, M., Schwab, C., Yu, S., McGeer, E., McGeer, P.L., 2009. Astrocytes produce the antiinflammatory and neuroprotective agent hydrogen sulfide. Neurobiol. Aging 30, 1523–1534. https://doi.org/10.1016/j.neurobiolaging.2009.06.001.

Liu, H., Radford, M.N., Yang, C. tao, Chen, W., Xian, M., 2018. Inorganic hydrogen polysulfides: chemistry, chemical biology and detection. Br. J. Pharmacol. 176, 616–627. https://doi.org/10.1111/bph.14330.

Mathai, J.C., Missner, A., Kügler, P., Saparov, S.M., Zeidel, M.L., Lee, J.K., Pohl, P., 2009. No facilitator required for membrane transport of hydrogen sulfide. Proc. Natl. Acad. Sci. U. S. A. 106, 16633–16638. https://doi.org/10.1073/pnas.0902952106.

McNamara, C.R., Mandel-Brehm, J., Bautista, D.M., Siemens, J., Deranian, K.L., Zhao, M., Hayward, N.J., Chong, J.A., Julius, D., Moran, M.M., Fanger, C.M., 2007. TRPA1 mediates formalin-induced pain. Proc. Natl. Acad. Sci. U. S. A. 104, 13525–13530. https://doi.org/10.1073/pnas.0705924104.

Miyamoto, R., Otsuguro, K., Ito, S., 2011. Time- and concentration-dependent activation of TRPA1 by hydrogen sulfide in rat DRG neurons. Neurosci. Lett. 499, 137–142. https://doi.org/10.1016/j.neulet.2011.05.057.

Mustafa, A.K., Gadalla, M.M., Sen, N., Kim, S., Mu, W., Gazi, S.K., Barrow, R.K., Yang, G., Wang, R., Snyder, S.H., 2009. H_2S signals through protein S-Sulfhydration. Sci. Signal. 2, 1–9. https://doi.org/10.1126/scisignal.2000464.

Nagai, Y., Tsugane, M., Oka, J., Kimura, H., 2004. Hydrogen sulfide induces calcium waves in astrocytes. FASEB J. 18, 557–559. https://doi.org/10.1096/fj.03-1052fje.

Navarrete, M., Perea, G., Maglio, L., Pastor, J., García De Sola, R., Araque, A., 2013. Astrocyte calcium signal and gliotransmission in human brain tissue. Cereb. Cortex 23, 1240–1246. https://doi.org/10.1093/cercor/bhs122.

Ogawa, H., Takahashi, K., Miura, S., Imagawa, T., Saito, S., Tominaga, M., Ohta, T., 2012. H_2S functions as a nociceptive messenger through transient receptor potential ankyrin 1 (TRPA1) activation. Neuroscience 218, 335–343. https://doi.org/10.1016/j.neuroscience.2012.05.044.

Peppiatt, C.M., Collins, T.J., Mackenzie, L., Conway, S.J., Holmes, A.B., Bootman, M.D., Berridge, M.J., Seo, J.T., Roderick, H.L., 2003. 2-Aminoethoxydiphenyl borate (2-APB) antagonises inositol 1,4,5-trisphosphate-induced calcium release, inhibits calcium pumps and has a use-dependent and slowly reversible action on store-operated calcium entry channels. Cell Calcium. 34, 97–108. https://doi.org/10.1016/S0143-4160(03)00026-5.

Perniss, A., Preiss, K., Nier, M., Althaus, M., 2017. Hydrogen sulfide stimulates CFTR in Xenopus oocytes by activation of the cAMP/PKA signalling axis. Sci. Rep. 7, 1–12. https://doi.org/10.1038/s41598-017-03742-5.

Pryazhnikov, E., Khiroug, L., 2008. Sub-micromolar increase in $[Ca^{2+}]_i$ triggers delayed exocytosis of ATP in cultured astrocytes. Glia. 56, 38–49. https://doi.org/ 10.1002/glia.20590.

Saleem, H., Tovey, S.C., Molinski, T.F., Taylor, C.W., 2014. Interactions of antagonists with subtypes of inositol 1,4,5-trisphosphate (IP_3) receptor. Br. J. Pharmacol. 171, 3298–3312. https://doi.org/10.1111/bph.12685.

Salter, M.W., Hicks, J.L., 1995. ATP causes release of intracellular Ca^{2+} via the phospholipase Cβ/IP_3 pathway in astrocytes from the dorsal spinal cord. J. Neurosci. 15, 2961–2971. https://doi.org/10.1523/jneurosci.15-04-02961.1995.

Salter, M.W., Hicks, J.L., 1994. ATP-evoked Increases in Intracellular Calcium in Neurons and Glia from the Dorsal Spinal Cord. J. Neurosci. 14, 1563–575.

https://doi.org/10.1523/JNEUROSCI.14-03-01563.1994.

Scemes, E., Giaume, C., 2006. Astrocyte calcium waves: What they are and what they do. Glia. 54, 716–725. https://doi.org/10.1002/glia.20374.

Szabo, C., Ransy, C., Módis, K., Andriamihaja, M., Murghes, B., Coletta, C., Olah, G., Yanagi, K., Bouillaud, F., 2014. Regulation of mitochondrial bioenergetic function by hydrogen sulfide. Part I. Biochemical and physiological mechanisms. Br. J. Pharmacol. 171, 2099–2122. https://doi.org/10.1111/bph.12369.

Testai, L., Marino, A., Piano, I., Brancaleone, V., Tomita, K., Di Cesare Mannelli, L., Martelli, A., Citi, V., Breschi, M.C., Levi, R., Gargini, C., Bucci, M., Cirino, G., Ghelardini, C., Calderone, V., 2016. The novel H_2S-donor 4-carboxyphenyl isothiocyanate promotes cardioprotective effects against ischemia/reperfusion injury through activation of mitoKATP channels and reduction of oxidative stress. Pharmacol. Res. 113, 290–299. https://doi.org/10.1016/j.phrs.2016.09.006.

Thastrup, O., Cullen, P.J., Drobak, B.K., Hanley, M.R., Dawson, A.P., 1990. Thapsigargin, a tumor promoter, discharges intracellular Ca^{2+} stores by specific inhibition of the endoplasmic reticulum Ca^{2+}-ATPase. Proc. Natl. Acad. Sci. U. S. A. 87, 2466–2470.

Trevisani, M., Patacchini, R., Nicoletti, P., Gatti, R., Gazzieri, D., Lissi, N., Zagli, G., Creminon, C., Geppetti, P., Harrison, S., 2005. Hydrogen sulfide causes vanilloid receptor 1-mediated neurogenic inflammation in the airways. Br. J. Pharmacol. 145,

1123–1131. https://doi.org/10.1038/sj.bjp.0706277.

Ujike, A., Otsuguro, K., Miyamoto, R., Yamaguchi, S., Ito, S., 2015. Bidirectional effects of hydrogen sulfide via ATP-sensitive K^+ channels and transient receptor potential A1 channels in RIN14B cells. Eur. J. Pharmacol. 764, 463–470. https://doi.org/10.1016/j.ejphar.2015.07.029.

Willmott, N.J., Wong, K., Strong, A.J., 2000. A fundamental role for the nitric oxide-G-kinase signaling pathway in mediating intercellular Ca^{2+} waves in glia. J. Neurosci. 20, 1767–1779. https://doi.org/10.1523/JNEUROSCI.20-05-01767.2000.

Yong, Q.C., Choo, C.H., Tan, B.H., Low, C.M., Bian, J.S., 2010. Effect of hydrogen sulfide on intracellular calcium homeostasis in neuronal cells. Neurochem. Int. 56, 508–515. https://doi.org/10.1016/j.neuint.2009.12.011.

Zalk, R., Lehnart, S.E., Marks, A.R., 2007. Modulation of the Ryanodine Receptor and Intracellular Calcium. Annu. Rev. Biochem. 76, 367–385. https://doi.org/10.1146/annurev.biochem.76.053105.094237.

Zhao, Z., Gordan, R., Wen, H., Fefelova, N., Zang, W.-J., Xie, L.-H., 2013. Modulation of Intracellular Calcium Waves and Triggered Activities by Mitochondrial Ca Flux in Mouse Cardiomyocytes. PLoS One 8, e80574. https://doi.org/10.1371/journal.pone.0080574.

Figure Legends

Fig. 1 H_2S increases $[Ca^{2+}]_i$ in spinal cord astrocytes.

(A) Representative $[Ca^{2+}]_i$ responses of four individual cells to Na_2S. (B) Peak amplitudes of the $[Ca^{2+}]_i$ increase after the application of Na_2S (0-150 μM, 10 min) (*n* = 89-100 cells from 3 cultures). (C) Effect of Na_2S (0−1000 μM) on LDH release. Astrocytes were treated with Na_2S for 6 h. The positive control (p.c.) indicates the results from lysed cells (*n* = 3). (D) Cell viability was assessed with MTT test. Astrocytes were treated with 150 μM Na_2S for 24 h (*n* = 5). Data are presented as means ± S.E.M. $^{\#\#}P < 0.01$ vs. 0 μM Na_2S (Dunnett's test)

Fig. 2 H_2S inhibits ATP-induced $[Ca^{2+}]_i$ increase in astrocytes.

(A) Representative $[Ca^{2+}]_i$ response to ATP (10 μM) in the absence (left) and presence of Na_2S (150 μM, right). ΔATP_1 is the difference of $[Ca^{2+}]_i$ between maximum value after the first application of ATP and the value just before that. ΔATP_2 is the difference of $[Ca^{2+}]_i$ between maximum value after the second application of ATP and the value just before that. (B) Peak amplitudes of the increase in $[Ca^{2+}]_i$ by Na_2S (0.1−150 μM, 10 min) after the first application of Na_2S (*n* = 97−136 cells from 3−4 cultures). (C) Summarized data of the ratio of the second ATP-induced $[Ca^{2+}]_i$ increase to the first one (*n* = 97−136 cells from 3−4 cultures). (D) Extracellular concentrations of ATP after the application of Na_2S (0.001−150 μM, 5 min) (*n* = 4). Data are presented as means ± S.E.M. $^{\#\#}P < 0.01$ vs. 0 μM Na_2S (Dunnett's test)

Fig. 3 Ca^{2+} response to H_2S does not depend on Ca^{2+} influx in spinal cord astrocytes.

(A) Effect of HC-030031 (10 μM, 2 min) on H_2S-induced $[Ca^{2+}]_i$ increase. ΔC_1 and ΔC_2 in the left trace indicate $[Ca^{2+}]_i$ before and after application of HC-030031, respectively. The amplitudes of ΔC_1 and ΔC_2 are summarized (right) (*n* = 74 cells from 4 cultures). (B) Effect of AITC (10 μM, 4 min) on $[Ca^{2+}]_i$ in the absence and presence of HC-030031 (10 μM). The same experiment was repeated four times (n = 121 cells from 4 cultures). (C) Effect of removal of the extracellular Ca^{2+} on H_2S-induced $[Ca^{2+}]_i$ increase. ΔC_1 and ΔC_2 in the left trace indicates $[Ca^{2+}]_i$ before and after removal of extracellular Ca^{2+}, respectively. The amplitude of ΔC_1 and ΔC_2 are summarized (right). (n = 94 cells from 4 cultures). Dotted lines indicate the basal $[Ca^{2+}]_i$ level (A, C). Data are presented as means ± S.E.M. *P < 0.05, **P < 0.01 vs. ΔC_1 (paired Student's t-test)

Fig. 4 H_2S induces Ca^{2+} release from the ER in astrocytes.

(A) Representative $[Ca^{2+}]_i$ responses to Na_2S (150 μM, 5 min) in the absence (left) and presence of thapsigargin (TG, 1 μM, right, 3 individual cells). (B) Peak amplitudes of the increased $[Ca^{2+}]_i$ by Na_2S under each condition are summarized (*n* = 67 [control (cont)], 76 [TG], and 99 cells [ryanodine (Rya)] from 3 cultures). (C) Representative $[Ca^{2+}]_i$ responses to ATP (10 μM, 30 sec). (D) Representative $[Ca^{2+}]_i$ responses to Na_2S (150 μM) after the second

application of ATP in the presence (left) and absence of extracellular Ca^{2+}(right). ΔATP_1 is the difference of $[Ca^{2+}]_i$ between maximum value after the first application of ATP and the value just before that. ΔATP_2 is the difference of $[Ca^{2+}]_i$ between maximum value after the second application of ATP and the value just before that. (E) Peak amplitudes of the increase in $[Ca^{2+}]_i$ by Na_2S (150 μM, 10 min) after the second application of ATP in the presence or absence of extracellular Ca^{2+} are summarized (*n* = 87 [control] and 76 [Ca^{2+} free] cells from 3 cultures). Data are presented as means ± S.E.M. $^{\#\#}P < 0.01$ vs. control (Dunnett's test), $^{**}P < 0.01$ vs. control (unpaired Student's t-test)

Fig. 5 *S*-sulfhydration and intracellular cAMP are not involved in the $[Ca^{2+}]_i$ increase by H_2S. (A) Effect of DTT (1 mM, 2 min) on $[Ca^{2+}]_i$ increase by Na_2S. ΔC_1 and ΔC_2 in the left trace indicates $[Ca^{2+}]_i$ before and after application of DTT, respectively. The amplitude of ΔC_1 and ΔC_2 are summarized (right) (*n* = 88 cells from 3 cultures). (B) Responses to ATP (10 μM, 30 s) in the absence or presence of Na_2S (150 μM) and/or DTT (1 mM). (C) Ratios of the second ATP-induced Ca^{2+} elevation to the first one are summarized. n.s., not significant (P = 0.42, unpaired Student's t-test) (*n* = 126 [control], 131 [DTT], 126 [Na_2S], and 123 [Na_2S + DTT] cells from 4 cultures). (D) Representative $[Ca^{2+}]_i$ responses to ATP (10 μM, 30 s) in the absence (left) or presence (right) of Na_2S_3 (10 μM). (E) Peak amplitudes of the $[Ca^{2+}]_i$ increase by Na_2S_3 (0.1−10 μM, 10 min) after the first application of ATP. (*n* = 116−134 cells

from 4 cultures). (F) Ratios of the second ATP-induced Ca^{2+} elevation to the first one in the presence of Na_2S_3 are summarized (n = 116−134 cells from 4 cultures). (G) The amount of cAMP per well after the application of Na_2S (150 μM), Na_2S_3 (10 μM), or forskolin (for, 100 μM) for 10 min (n = 3). Data are presented as means ± S.E.M. **P < 0.01 (paired Student's t-test), $^{\#}$P < 0.05, $^{\#\#}$P < 0.01 vs. 0 μM Na_2S (Dunnett's test)

Fig. 1

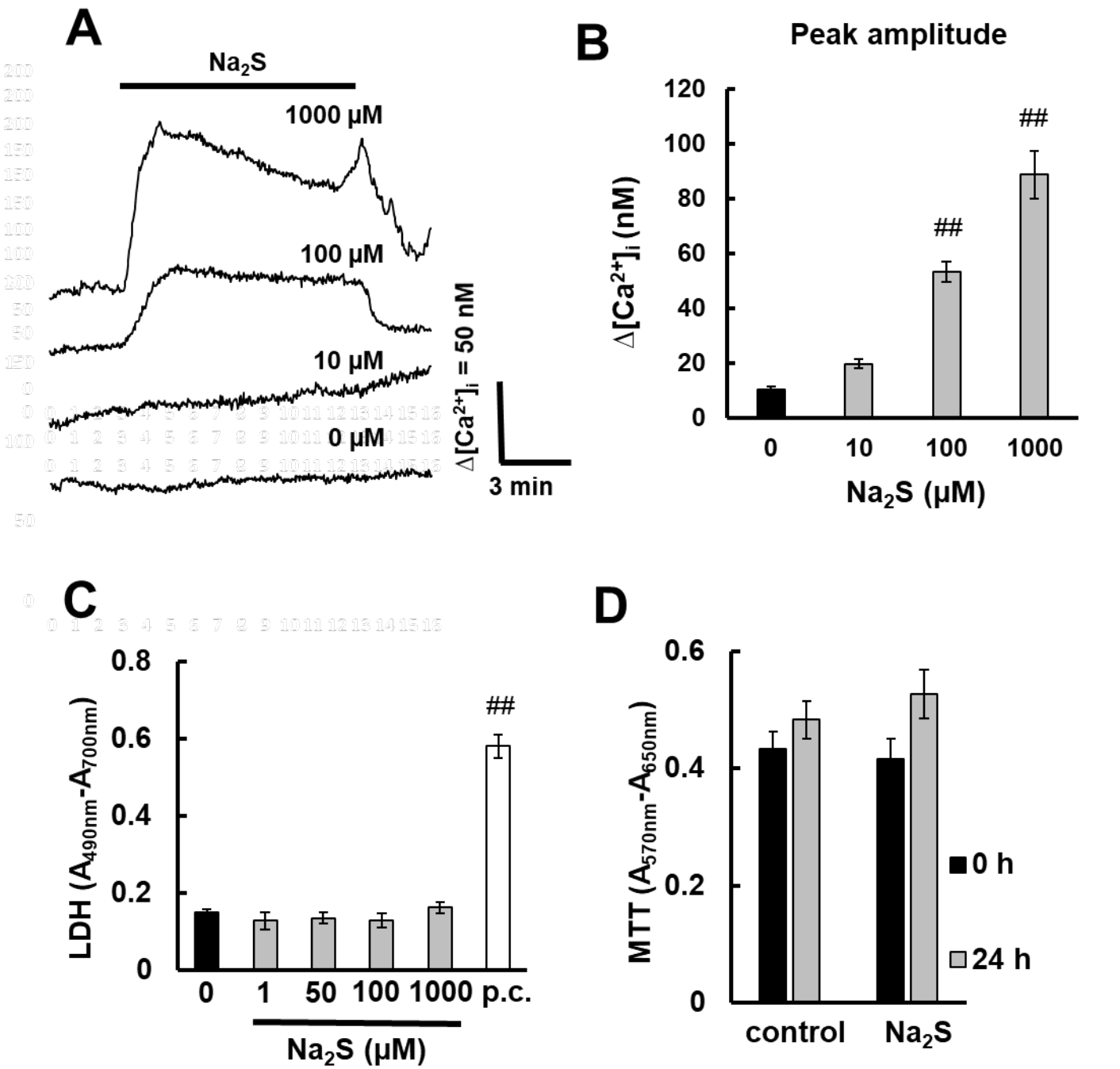
A
Na2S
1000 μM
100 μM
10 μM
0 μM
Δ[Ca2+]i = 50 nM
3 min
B
Peak amplitude
Δ[Ca2+]i (nM)
##
##
0
10
100
1000
Na2S (μM)
C
LDH (A490nm-A700nm)
##
0
1
50
100
1000
p.c.
Na2S (μM)
D
MTT (A570nm-A650nm)
0 h
24 h
control
Na2S

Fig. 2

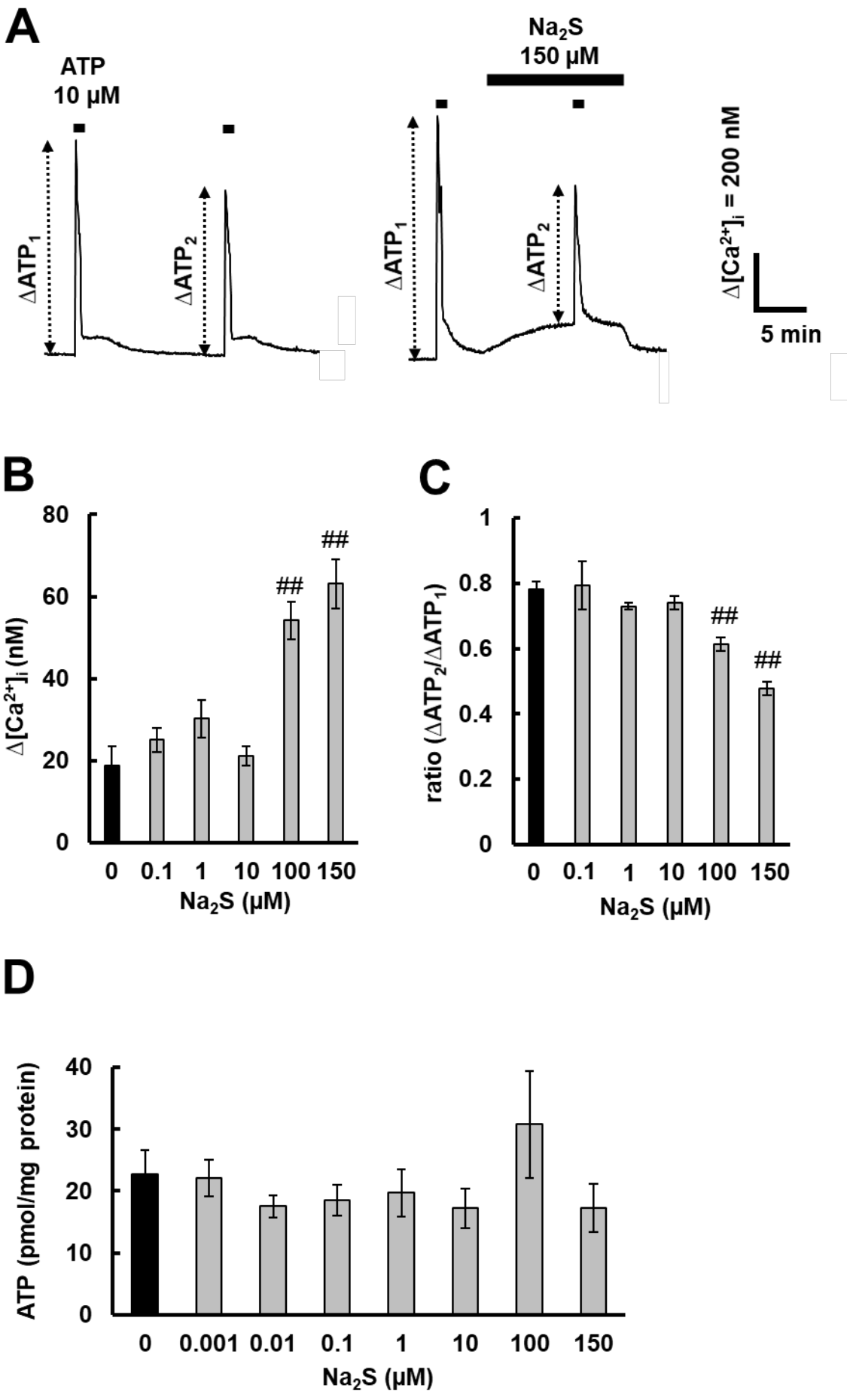
A
ATP
10 μM
Na2S
150 μM
ΔATP1
ΔATP2
Δ[Ca2+]i = 200 nM
5 min
B
Δ[Ca2+]i (nM)
##
0 0.1 1 10 100 150
Na2S (μM)
C
ratio (ΔATP2/ΔATP1)
##
0 0.1 1 10 100 150
Na2S (μM)
D
ATP (pmol/mg protein)
0 0.001 0.01 0.1 1 10 100 150
Na2S (μM)

Fig. 3

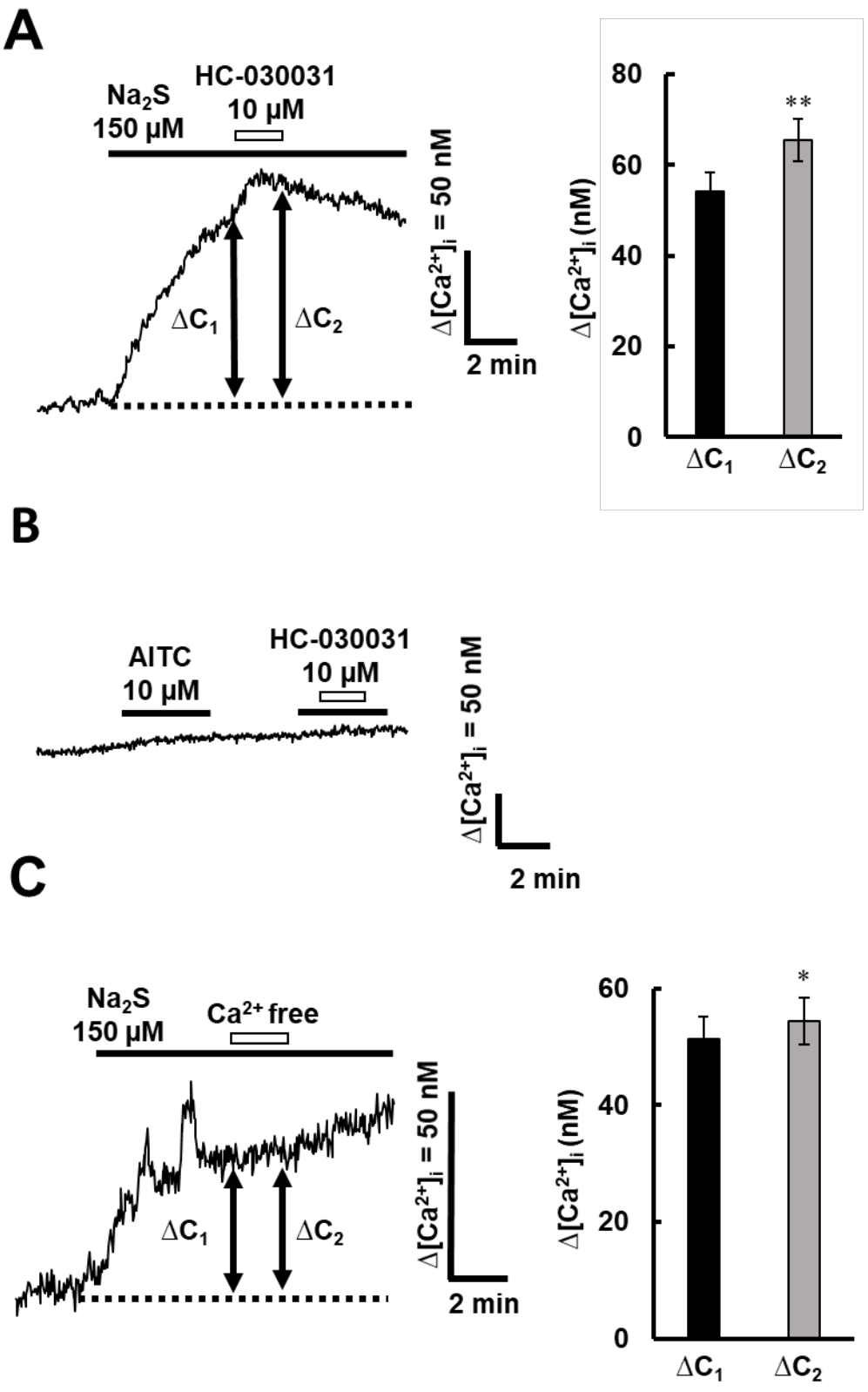
A
Na2S
150 μM
HC-030031
10 μM
ΔC1
ΔC2
Δ[Ca2+]i = 50 nM
2 min
Δ[Ca2+]i (nM)
80
60
40
20
0
**
ΔC1
ΔC2
B
AITC
10 μM
HC-030031
10 μM
Δ[Ca2+]i = 50 nM
2 min
C
Na2S
150 μM
Ca2+ free
ΔC1
ΔC2
Δ[Ca2+]i = 50 nM
2 min
Δ[Ca2+]i (nM)
60
40
20
0
*
ΔC1
ΔC2

Fig. 4

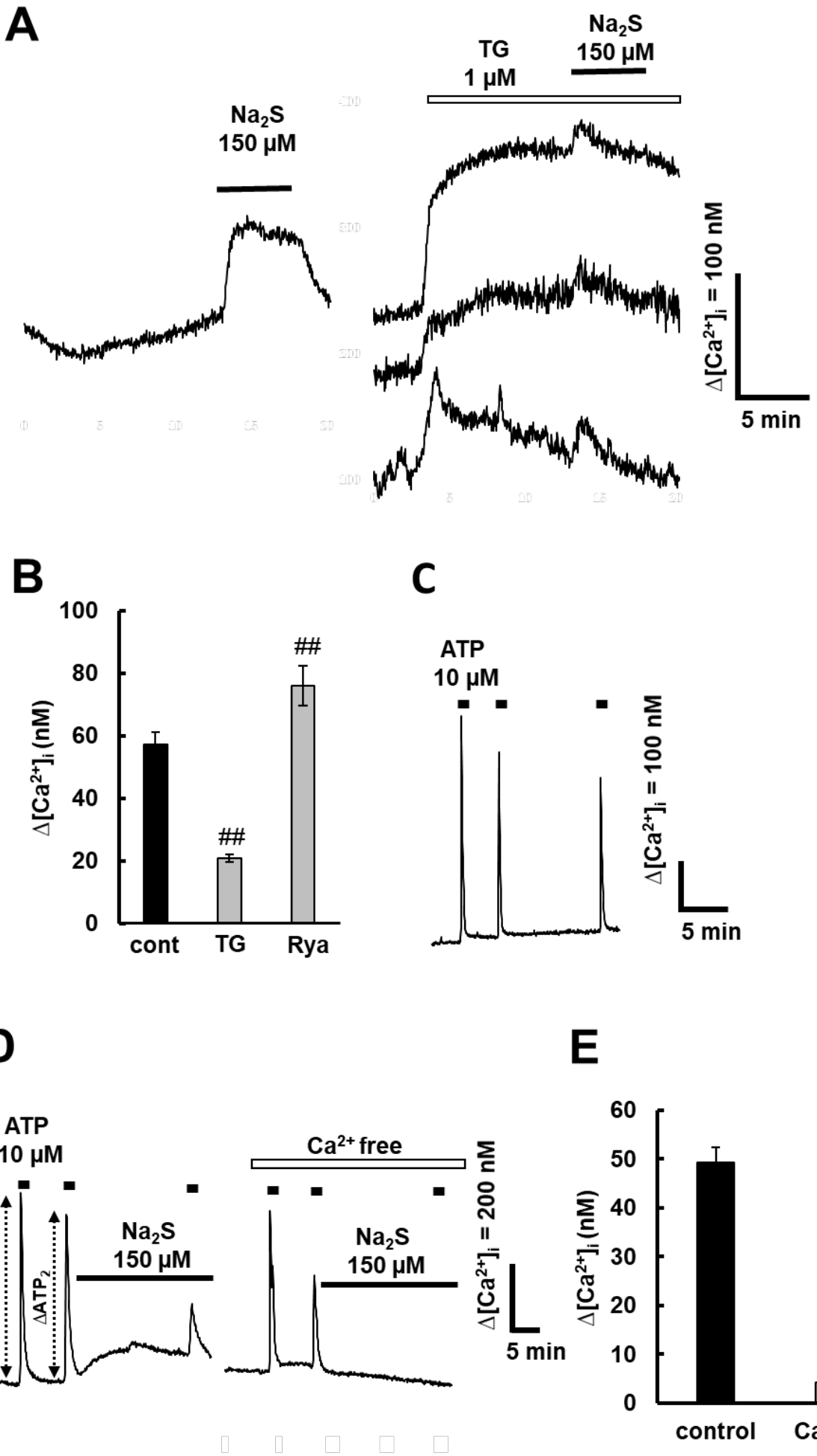
A
Na2S
150 μM
TG
1 μM
Na2S
150 μM
Δ[Ca2+]i = 100 nM
5 min
B
Δ[Ca2+]i (nM)
100
80
60
40
20
0
##
##
cont
TG
Rya
C
ATP
10 μM
Δ[Ca2+]i = 100 nM
5 min
D
ATP
10 μM
Ca2+ free
Na2S
150 μM
Na2S
150 μM
ΔATP1
ΔATP2
Δ[Ca2+]i = 200 nM
5 min
E
Δ[Ca2+]i (nM)
60
50
40
30
20
10
0
**
control
Ca free

Fig. 5

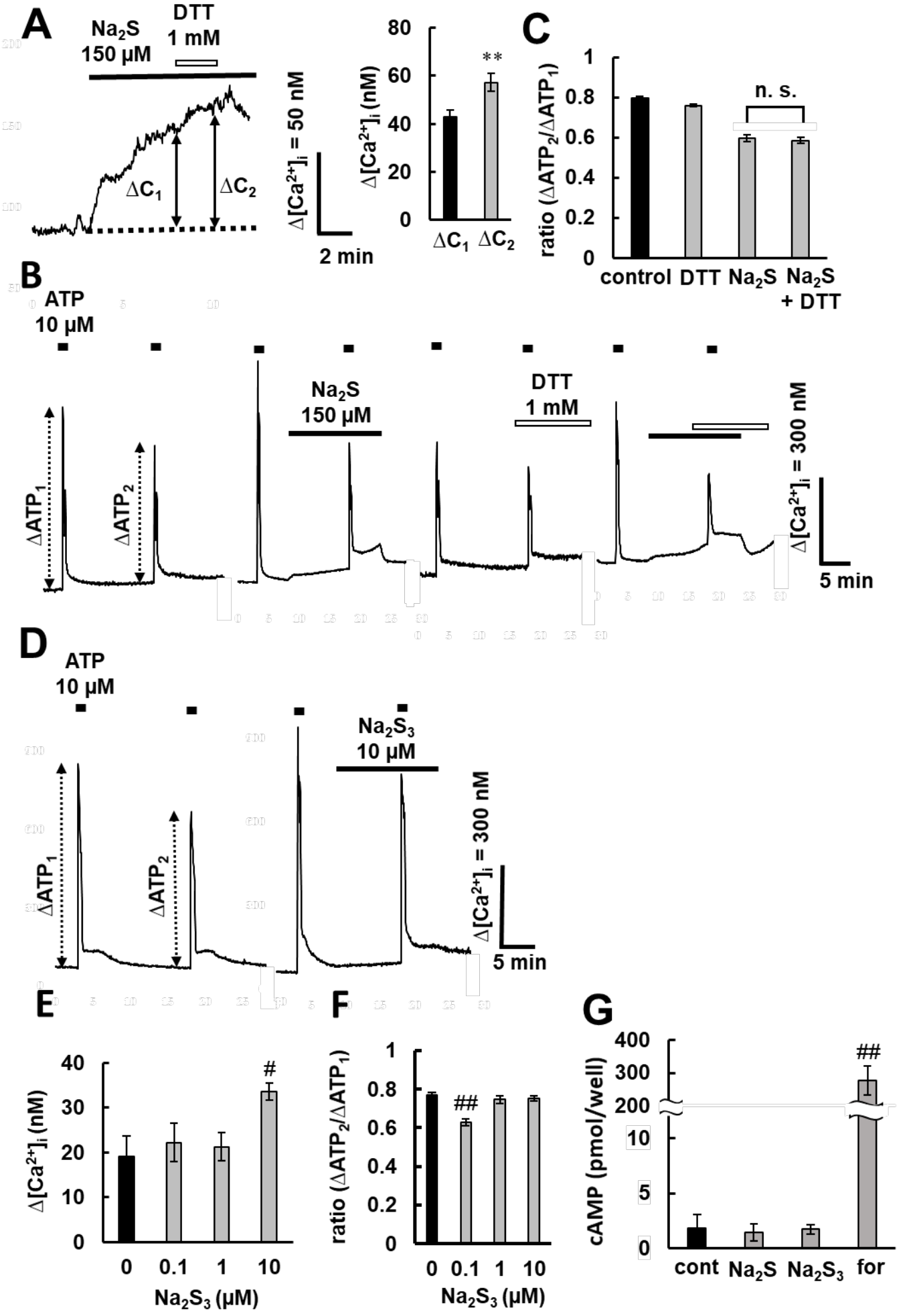
A
Na2S
150 μM
DTT
1 mM
ΔC1
ΔC2
Δ[Ca2+]i = 50 nM
2 min
Δ[Ca2+]i (nM)
**
ΔC1 ΔC2
C
ratio (ΔATP2/ΔATP1)
n. s.
control DTT Na2S Na2S + DTT
B
ATP
10 μM
Na2S
150 μM
DTT
1 mM
ΔATP1
ΔATP2
Δ[Ca2+]i = 300 nM
5 min
D
ATP
10 μM
Na2S3
10 μM
ΔATP1
ΔATP2
Δ[Ca2+]i = 300 nM
5 min
E
Δ[Ca2+]i (nM)
#
0 0.1 1 10
Na2S3 (μM)
F
ratio (ΔATP2/ΔATP1)
##
0 0.1 1 10
Na2S3 (μM)
G
cAMP (pmol/well)
##
cont Na2S Na2S3 for

supplementary Fig. 1

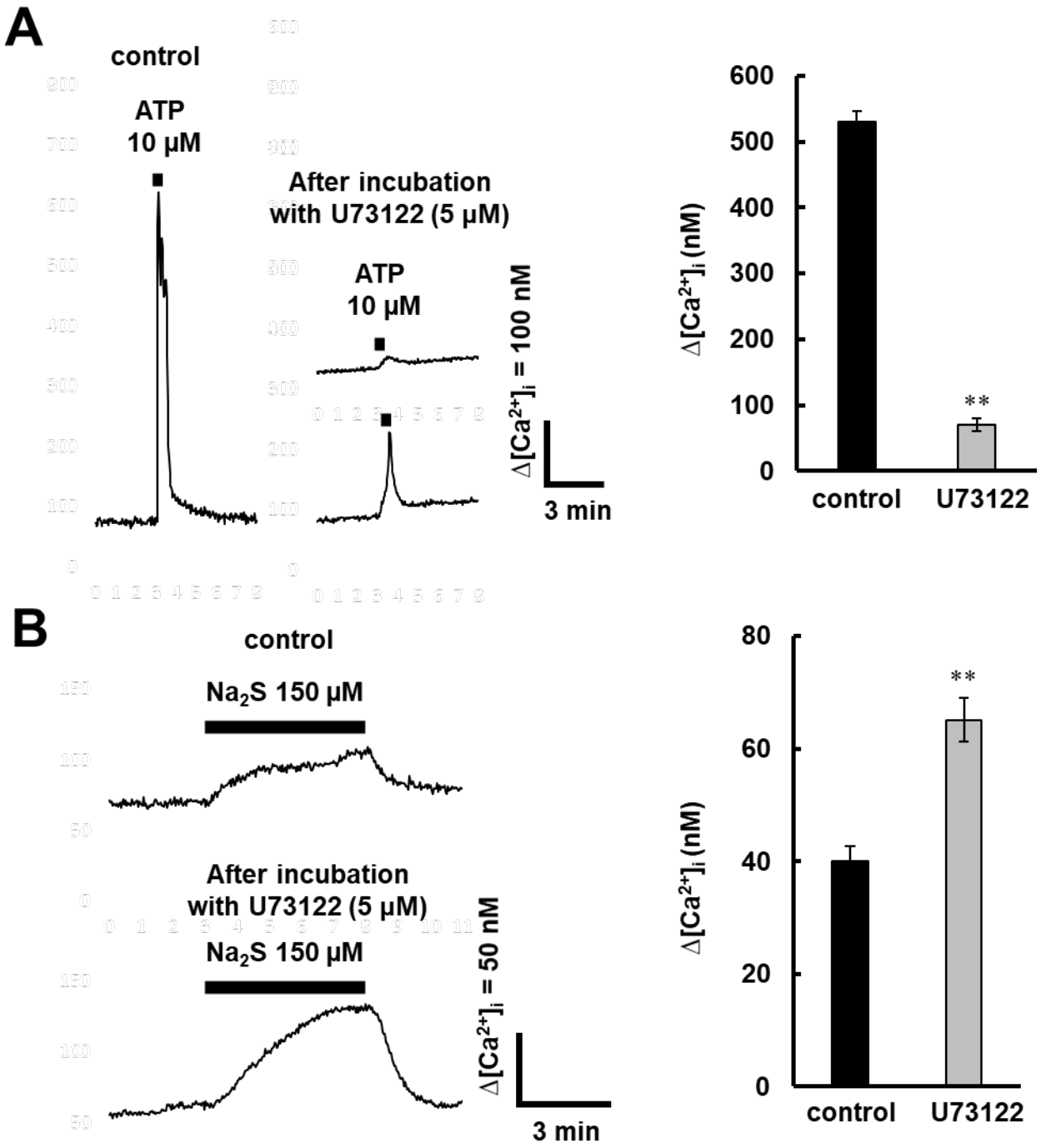

Supplementary Fig. 1 ATP induces $[Ca^{2+}]_i$ increase mainly through IP_3 signaling pathway. Representative $[Ca^{2+}]_i$ response to ATP (10 μM, 30 s, A) or Na_2S (150 μM, 5 min, B) after incubation with or without U73122 (5 μM, 60 min, left). The maximum amplitude of $[Ca^{2+}]_i$ increase are summarized (right). (ATP, n = 81 [control] and 89 [U73122] cells from 3 cultures. Na_2S, n = 87 [control] and 87 [U73122] cells from 3 cultures). Data are presented as means ± S.E.M. **P < 0.01 vs. control (unpaired Student's t-test)

supplementary Fig. 2

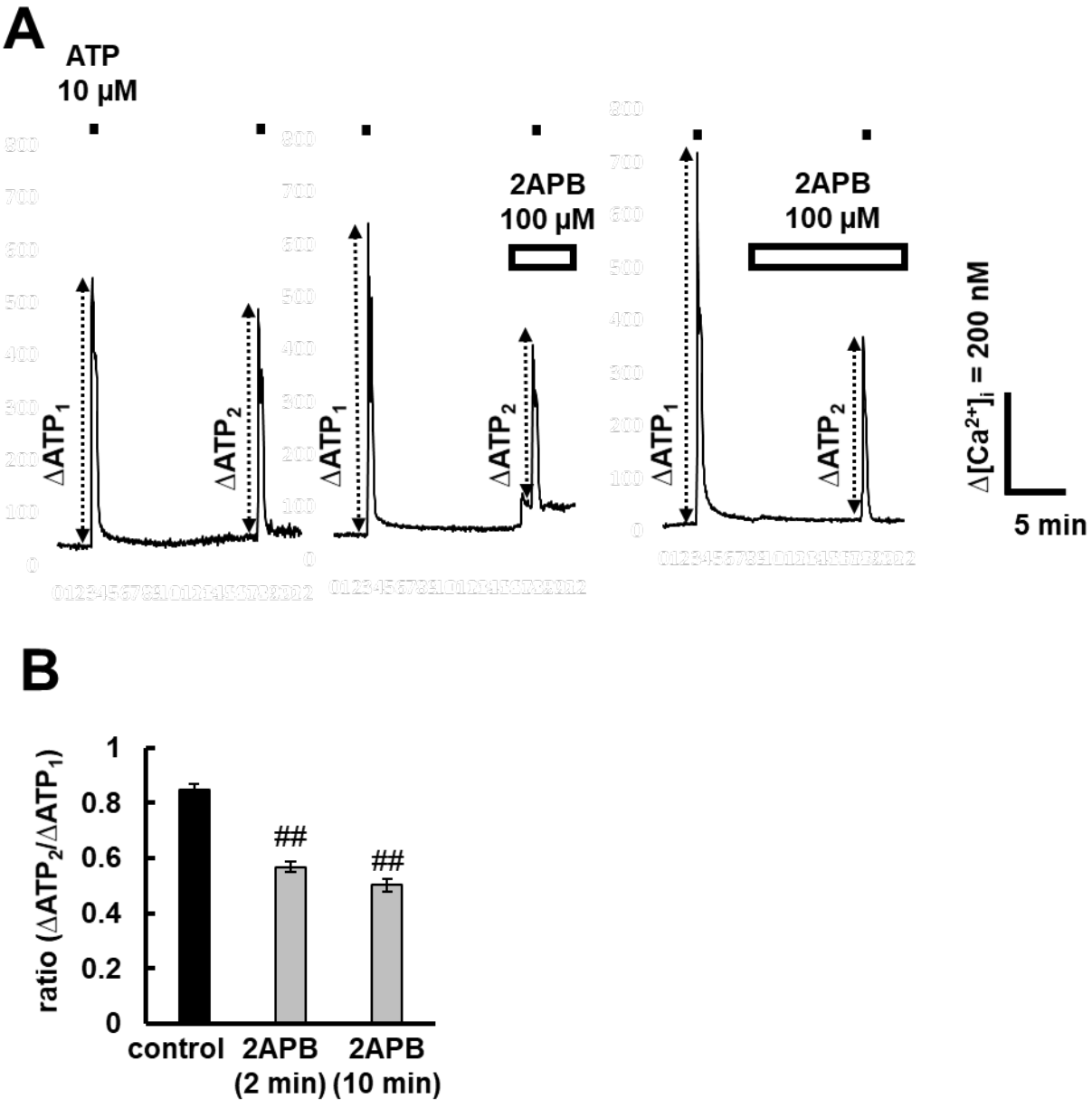

Supplementary Fig. 2 2APB did not completely inhibit ATP-induced Ca^{2+} response in spinal cord astrocytes. (A**)** Responses to ATP (10 μM, 30 s) after incubation with or without 2APB (100 μM, 2 or 10 min). (B**)** Ratios of the second ATP-induced Ca^{2+} elevation to the first one are summarized. (n = 80 [control], 92 [2APB 2 min], and 92 [2APB 10 min] cells from 3 cultures). Data are presented as means ± S.E.M. $^{\#\#}P < 0.01$ vs. control (Dunnett's test)

supplementary Fig. 3

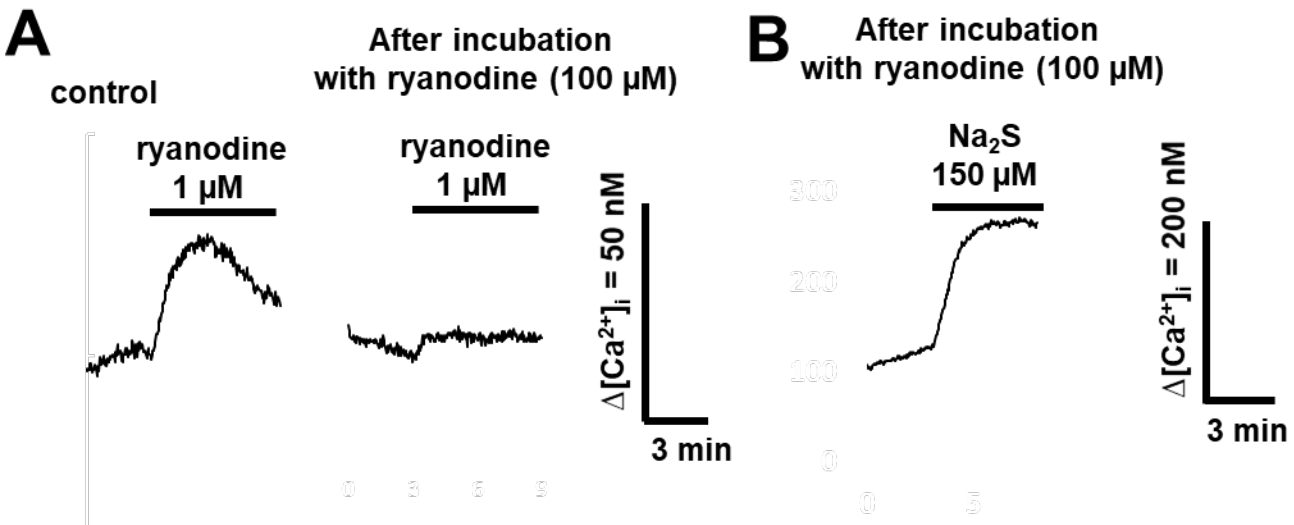

Supplementary Fig. 3 Ryanodine receptors are not involved in the $[Ca^{2+}]_i$ increase by H_2S. (A) Representative $[Ca^{2+}]_i$ response to ryanodine (1 μM) after incubation with or without ryanodine (100 μM, 30 min). At the end of these experiments, we confirmed the existence of Ca^{2+} in the ER by ATP (10 μM)-induced $[Ca^{2+}]_i$ increase. (B) Representative $[Ca^{2+}]_i$ response to Na_2S (150 μM, 5 min) after incubation with ryanodine (100 μM, 30 min). The same experiment was repeated three times (n = 99 cells from 3 cultures).